Machine learning-based risk stratification of patients with heart failure

Ph.D. Thesis

Márton Tokodi, M.D.

Doctoral School of Basic and Translational Medicine
Semmelweis University

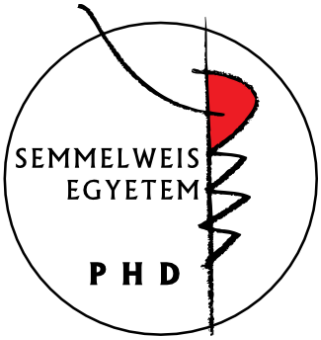

Supervisor: Attila Kovács, M.D., Ph.D.

Official reviewers: András Horváth, Ph.D.

Pál Kaposi Novák, M.D., Ph.D.

Head of the Complex Examination Committee:

István Karádi, M.D., D.Sc.

Members of the Complex Examination Committee:

Lívia Jánoskuti, M.D., Ph.D.

József Borbola, M.D., Ph.D.

Budapest
2021

1. INTRODUCTION

With data-rich technologies and data-heavy areas of biomedical science entering the clinical arena, physicians are being inundated with a staggering volume of data requiring more sophisticated interpretation while being expected to perform more efficiently. In other words, the ever-growing complexity of medicine now exceeds the capacity of the human mind. A potential solution is machine learning (ML) – a subfield of artificial intelligence – that can support clinical decision-making to enhance every stage of patient care.

ML algorithms can account for non-linear associations between myriads of predictors and outcomes; thus, their utilization will inevitably lead to improved predictive models. As ML-based tools permeate into clinical cardiology, they will facilitate the scheduling and protocolling of medical tests and appointments, help remote monitoring of patients through wearable devices, enhance the interpretation of electrocardiograms (ECGs), enable automated measurements from echocardiograms, computed tomography, and cardiac magnetic resonance scans, perform risk stratification using every piece of data available in the patient's chart, and guide therapeutic decisions. Designed, validated, and implemented appropriately, ML models will help us acquire, interpret, and synthesize healthcare data from diverse sources and place it at our fingertips.

ML also holds the promise to revolutionize heart failure (HF) care and ultimately improve outcomes in this patient population. ML has been leveraged in an attempt to facilitate the diagnosis of HF, the classification of HF patients into subgroups requiring different treatment strategies, and the prognostication of HF patients in order to deliver more tailored care. ML techniques can be applied in other aspects of the management of HF as well. For instance, they can predict whether the patient will adhere to the prescribed medications or identify HF patients at risk of depression. ML can also be employed to predict left ventricular (LV) filling pressures or to protect cardiovascular implantable electronic devices from cyberattacks. Although these are only cherry-picked use cases, they make it apparent that ML can be successfully applied for countless prediction tasks related to HF.

Accordingly, the potentials of ML were demonstrated in this thesis through three studies aiming to improve the prognostication of HF patients.

2. OBJECTIVES

1. **Applying topological data analysis to integrate echocardiographic features of left ventricular structure and function into a patient similarity network**

A diagnostic imaging protocol can produce numerous parameters, each with its strengths and limitations. However, due to the lack of unanimity on the combination and use of these parameters to depict a single patient or a group of patients with similar characteristics, there is a paramount need to develop a staging method that can integrate multiple tests and diagnostic variables at the point of care. Accordingly, we applied topological data analysis (TDA) to detect patient similarity patterns using a cross-sectional multi-parametric echocardiographic data set. We subsequently investigated the prognostic value of the topological network and explored whether the longitudinal course of the disease could be tracked along the topological map to assess the risk of cardiac events in an index patient.

2. **Designing and evaluating a machine learning-based risk stratification system to predict all-cause mortality of patients undergoing CRT implantation**

Cardiac resynchronization therapy (CRT) decreases morbidity and mortality in appropriately selected patients, yet some patients show limited or no response to therapy. Since this discovery, interest has spiked in attempting to accurately risk-stratify this patient population; however, conventional statistics-based risk scores have achieved only modest performance. Therefore, we implemented an ML-based risk stratification system to predict all-cause mortality from pre-implantation parameters of patients undergoing CRT implantation.

3. **Exploring the sex-specific differences and similarities in the predictors of mortality among patients undergoing CRT implantation**

In HF with reduced ejection fraction (HFrEF), several studies have highlighted sex-related differences that involve multiple aspects of the syndrome. Although sex disparities are also remarkable in the accessibility to HF device therapy, including CRT, women are more likely to respond favorably and derive a greater survival benefit from CRT implantation. Nonetheless, the sex-related differences in short- and long-term outcomes and the varying importance of different predictors are still scarcely explored in this patient population. Motivated by this gap in knowledge, we aimed to explore the sex-specific differences and similarities in the predictors of mortality using advanced ML-based approaches.

3. METHODS

3.1 Study population and methods of investigating interpatient similarities using topological data analysis

3.1.1 Outline of the study protocol

Our study consisted of two parts. First, we used a primary cohort (including patients from a retrospective study and two prospective registries) to create a cross-sectional representation of patients across different stages of cardiac disease. After we developed a topological network from the retrospective study, we added the data from the prospective registries to validate the persistence and stability of network topology. Second, we tested whether we could perform personalized predictions for a previously unseen group of patients (secondary cohort) who had two echocardiographic evaluations. As these patients underwent two echocardiographic examinations, the change in their location on the network was also monitored to investigate whether the network could represent the changes in cardiac disease staging. The institutional review board approved the study protocol, and all study participants in the prospective studies provided written informed consent.

3.1.2 Study population

The retrospective group included 866 outpatients (65 ± 17 years, 44.7% males) referred for transthoracic echocardiographic examination between March 2013 and December 2015 at the Icahn School of Medicine at Mount Sinai (New York, New York). The prospective group included 468 patients (55 ± 15 years, 41.7% males) enrolled between July 2017 to February 2018 in two ongoing patient registries at West Virginia University (Morgantown, West Virginia) that followed two prospective trials (NCT02560168 and NCT02248831). The pooled patients from the retrospective study and the two prospective registries formed the primary cohort, which was used for developing the patient-patient similarity network.

For personalized patient predictions, we tested the topological model in 96 additional patients (secondary cohort, 58 ± 15 years, 51.0% males) who had two consecutive echocardiographic examinations. Follow-up data for this cohort were collected after the second echocardiographic assessment.

3.1.3 Topological data analysis

TDA was performed using the cloud-based Ayasdi Workbench (version 7.4, Ayasdi Inc., Menlo Park, CA). Nine echocardiographic variables were used to create the topological network, namely, LV ejection fraction (LVEF), LV mass index, early (E) and late (A) diastolic transmitral flow velocities, E/A ratio, early diastolic relaxation velocity (e'), E/ e' ratio, left atrial volume index, and tricuspid regurgitation peak velocity (TRV). Data were analyzed using a normalized correlation metric with two multi-dimensional scaling lenses (resolution: 66, gain: 2.7, equalized). In the created topological network, each node represented a cluster of patients, whereas edges connected nodes that had at least one patient in common. Nodes were color-coded based on the average value of the parameter of interest (e.g., LVEF).

After creating the network in the primary cohort, we divided it into four regions for further analyses. We trained a random forest-based classifier using the echocardiographic data of the primary cohort to predict the region that each patient of the secondary cohort might belong to.

3.1.4 Clinical outcomes, endpoints, and staging

Patient electronic medical records were reviewed for post-echocardiographic follow-up. Endpoints were death from a major adverse cardiac event (MACE, defined as myocardial infarction, acute coronary syndrome, acute decompensated HF, cardiac arrest, or arrhythmia) and first MACE-related rehospitalization. The time to each endpoint was measured from the date of the echocardiographic examination used in the study. Clinical cardiac disease staging was performed using New York Heart Association (NYHA) functional class assessment, American College of Cardiology (ACC) / American Heart Association (AHA) HF staging, and the Meta-Analysis Global Group in Chronic Heart Failure (MAGGIC) risk score.

3.2 Study population and methods of machine learning-based mortality prediction among patients undergoing CRT implantation

3.2.1 Study population and protocol

We identified 2,282 patients who underwent successful CRT implantation at the Heart and Vascular Center of Semmelweis University (Budapest, Hungary) between September 2000 and December 2017. For each patient, pre-implantation clinical characteristics such as demographics, medical history, physical status, and vitals, currently applied medical therapy,

ECG, echocardiographic, and laboratory parameters were extracted retrospectively from electronic medical records and entered into our structured database.

An additional prospective database of patients undergoing CRT implantation between January 2009 and December 2011 was also utilized. Patients included in both the retrospective and the prospective databases were removed from the retrospective database. In this way, the two cohorts were completely independent, and they could be used as training and test cohorts for ML algorithms.

The study protocol complies with the Declaration of Helsinki, and it was approved by the Regional and Institutional Committee of Science and Research Ethics (approval No. 161/2019).

3.2.2 Feature selection and data pre-processing

Our structured database initially comprised over 100 easily obtainable pre-implantation clinical variables. Firstly, features included in both the retrospective and the prospective databases were identified (n = 49). Then, features missing for >40% of cases (n = 16) were excluded. The final set of input features included 33 pre-implantation clinical variables.

Missing values were imputed using the mean imputation method, which replaces the missing values of a certain variable with the mean of the available cases. As the range of different features varied widely and some of the utilized algorithms required the data to be normalized, Z-score transformation was performed after imputation.

3.2.3 Model development

We used the follow-up data to generate six classes of possible outcomes: death during the 1st (class 1), the 2nd (class 2), the 3rd (class 3), the 4th (class 4), the 5th year after CRT implantation (class 5), and no death during the first 5 years following the implantation (class 6). The task of ML algorithms was to predict the class membership probabilities of each patient over these classes based on the pre-implantation clinical features.

Model development included trials of several ML classifiers such as logistic regression, ridge regression, support vector machine (SVM), k-nearest neighbors (KNN) classifier, gradient boosting classifier, traditional random forest (TRF), conditional inference random forest (CIRF), and multi-layer perceptron. Models were trained with stratified 10-fold cross-validation on the training cohort, and a grid search approach was used to tune the hyper-parameters of each ML algorithm.

The outputs of each model were series of six values representing the previously defined class membership probabilities. To create binary classifiers, we calculated cumulative class membership probabilities by summing these values until the given year of follow-up. The computed cumulative probabilities were then calibrated using Platt's scaling, and the survival curve could be plotted for each patient. To quantify the model's discriminative capabilities in each year, receiver operating characteristic (ROC) curve analysis was performed, and the area under the ROC curve (AUC) was calculated. The mean AUC of 1-, 2-, 3-, 4-, and 5-year calibrated cumulative probabilities was computed, and it served as the major metric to assess a model's performance.

3.2.4 Model testing

The model with the highest mean AUC was selected for further evaluation, and it is referenced as the SEMMELWEIS-CRT (perSonalizEd assessMent of estiMatEd risk of mortaLity With machinE learnIng in patientS undergoing CRT implantation) score throughout the entire thesis. To determine whether the model remains accurate when new data are fed into it, we tested it on the patients of the test cohort. For each patient in the test cohort, we also computed pre-existing risk scores (Seattle Heart Failure Model [SHFM], VALID-CRT, EAARN, ScREEN, and CRT-score). Their prediction capabilities were quantified annually with AUCs, and they were compared with SEMMELWEIS-CRT score using the DeLong test.

3.3 Study population and methods of exploring sex-specific patterns of mortality predictors among patients undergoing CRT implantation

3.3.1 Study population and protocol

We identified 2,412 patients with chronic HFrEF (NYHA functional class II-IV) who underwent successful CRT implantation at the Heart and Vascular Center of Semmelweis University (Budapest, Hungary) between September 2000 and September 2018. For each patient, pre-implantation clinical characteristics (demographics, medical history, physical status, vitals, currently applied medical therapy, ECG, echocardiographic and laboratory parameters) and procedural parameters (type of the implanted device, LV lead position) were collected retrospectively from paper-based or electronic medical records and entered to our structured database. The study protocol complies with the Declaration of Helsinki, and it was approved by the Regional and Institutional Committee of Science and Research Ethics (Approval No. 161/2019).

3.3.2 Study outcomes

Follow-up data (status [dead or alive], date of death) was obtained for all patients by querying the National Health Insurance Database of Hungary in September 2019. Accordingly, all patients included in our database were followed for at least 1 year or died within 1 year. In the entire study population, 2,116 patients also had 3-year outcome data available. The primary endpoint of our study was all-cause mortality.

3.3.3 Feature selection and data pre-processing

Feature selection included two consecutive steps. First, any feature with ≥40% missing data was removed. Second, collinear variables (Spearman correlation coefficient ≥ 0.3 or ≤-0.3) were also excluded as variables containing redundant information might bias the further steps of the analysis. The final set of input features comprised 30 pre-implantation and procedural variables. Patients with more than 30% of missing values were excluded from further analyses. Missing values of continuous variables were imputed using multiple imputation by chained equations (MICE). Missing values of categorical variables were replaced with -1. As the range of different continuous features varied widely, Z-score transformation was applied after imputation to eliminate the possibility of model bias caused by the differing magnitude of the numerical values.

3.3.4 Model development and evaluation

We developed ML models to predict two separate outcomes: (1) 1-year all-cause mortality, and (2) 3-year all-cause mortality in the entire cohort, in males and females separately (a total of 6 separate binary classification tasks). To quantify a model's discriminatory power, ROC curve analysis was performed, and the AUC was calculated. Model development included trials of several binary classifiers such as logistic regression, SVM, KNN, Gradient Boosting classifier, TRF, CIRF, and multi-layer perceptron.

As the first step of model derivation, 20% of the given patient subset (all patients, males or females) was randomly selected as the holdout (test cohort). Hyperparameter tuning was performed with stratified 10-fold cross-validation in the remaining data (80%, training cohort). The algorithm (with fine-tuned hyperparameters) exhibiting the highest AUC was then retrained in the entire training cohort, and its performance was evaluated in the test cohort in a statistically independent way.

3.3.5 Feature importances

To determine the major predictors of 1- and 3-year all-cause mortality in each patient subset, permutation feature importances were computed from each of the 6 final models. Briefly, the importance of an input feature is measured by calculating the increase in the model's prediction error after permuting its values while keeping other features the same as before. In the current study, permutation was performed 10 times for each feature. A feature is considered important if shuffling its values decreases the model's discriminatory power (AUC) as the model relies heavily on that feature for the prediction. On the other hand, a feature is unimportant if shuffling its values leaves the AUC unchanged because, in this case, the model ignores the feature while predicting the outcome. After calculating the importance of each feature, we divided it by the AUC measured in the data set before shuffling any of its features to enable the comparison of feature importances between different models.

3.4 Statistical analysis and software packages

Continuous variables are expressed as median (interquartile range), while categorical variables are reported as frequencies and percentages. Between-group comparisons were performed using unpaired Student's t-test, Mann-Whitney U test, Kolmogorov-Smirnov test, analysis of variance, or Kruskal-Wallis test for continuous variables, and Chi-squared test or Fisher's exact test for categorical variables, as appropriate. Correlations between categorical variables were computed using Goodman and Kruskal's γ coefficient. The survival of subgroups was visualized using Kaplan-Meier curves, and Log-rank tests were performed for comparison. Cox proportional hazards models were used to compute hazard ratios (HRs) with 95% confidence intervals (CIs). A p-value of <0.05 was considered statistically significant.

Data pre-processing, feature selection, and ML algorithms were implemented in Python (version 3.6.7 and 3.6.8, Python Software Foundation, Wilmington, Delaware, USA) using the scikit-learn library (versions 0.20.2, 0.21.3, and 0.23.dev0). Statistical analyses, including group comparisons and survival analyses, were performed in R (versions 3.4.0, 3.4.2, and 3.6.1, R Foundation for Statistical Computing, Vienna, Austria).

4. RESULTS

4.1 Applying topological data analysis to integrate echocardiographic features of left ventricular structure and function into a patient similarity network

4.1.1 The continuum of cardiac function

The use of TDA to create a patient-patient similarity network in the retrospective data set resulted in the formation of a looped structure (Figure 1). After the addition of cases from the prospective data set, the loop was persistent, which validated that the loop structure of the network model was intrinsic to the data and not an artifact. The combined network was used for discovering feature distributions and developing associations with clinical and outcome data. With progressing from the 1st to the 4th region, an increasing trend was seen in age and the prevalence of cardiovascular risk factors. We also noted that echocardiographic variables followed a gradually changing pattern throughout the loop. LVEF remained preserved in regions I-III; however, it was significantly reduced in the 4th region ($p < 0.001$). LV mass progressively increased, and the parameters of diastolic function progressively worsened from region I to IV. We found a correlation between the regions and both NYHA functional classes ($\gamma = 0.47$; $p < 0.001$) and ACC/AHA stages ($\gamma = 0.52$; $p < 0.001$) in the prospective cohort.

4.1.2 The association of regions with major adverse cardiac events

The median follow-up time in the primary cohort was 309 (100 – 531) days. A total of 207 (16%) patients experienced MACE-related hospitalizations, and 19 (1%) patients died due to MACE during follow-up. The number of MACE-related hospitalizations increased progressively from regions I to IV ($p < 0.001$), with MACE-related deaths seen only in the 3rd and 4th regions ($p < 0.001$). The Kaplan-Meier curves for MACE-related rehospitalization in the regions differed significantly ($p < 0.001$) (Figure 2A). The number of MACE-related deaths was low in the 1st and 2nd regions, whereas the probability of death was significantly higher in the 3rd and 4th regions than in the 1st region ($p < 0.001$) (Figure 2B).

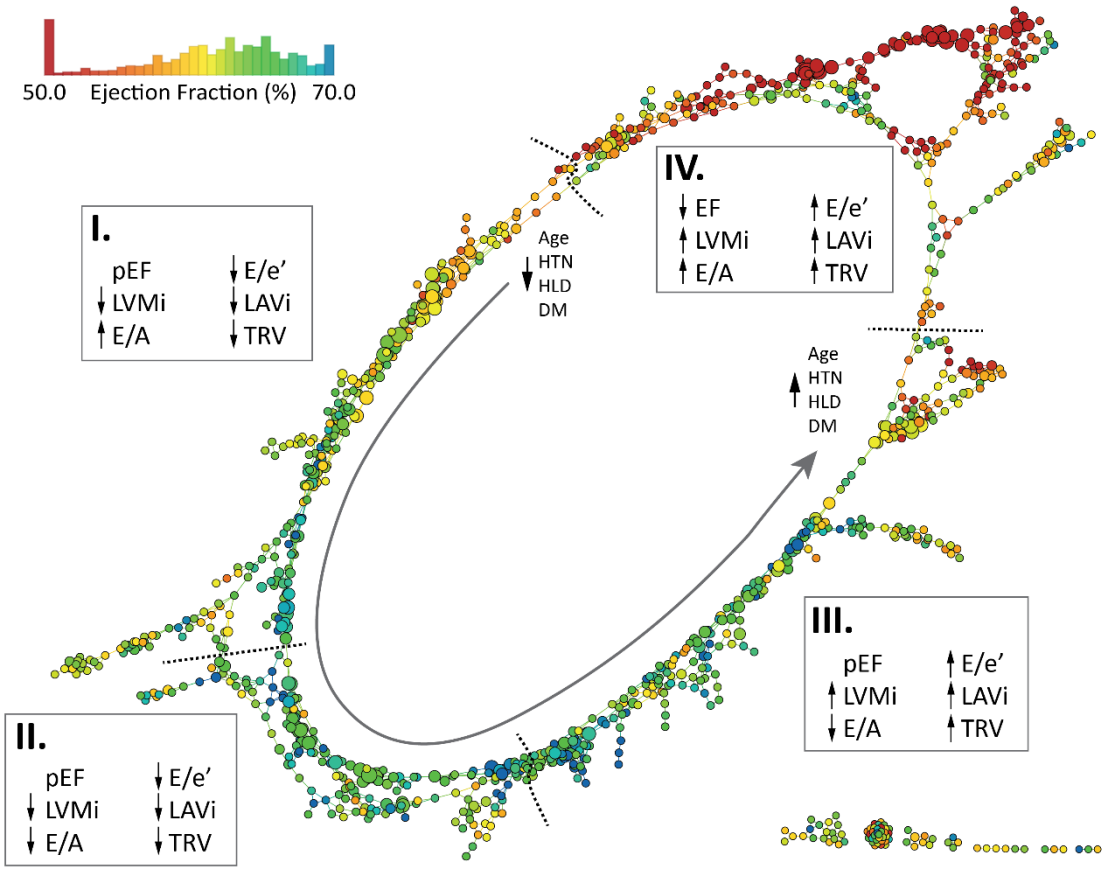

Figure 1 *The looped network of cardiac dysfunction*

Nodes indicate one or more patient(s) who have similar echocardiographic characteristics, and nodes having at least one patient in common are connected by edges. Nodes were color-coded according to the mean EF of the patients in the given node.

A – late diastolic transmitral flow velocity, DM – diabetes mellitus, E – early diastolic transmitral flow velocity, e' – early diastolic relaxation velocity at septal mitral annular position, EF – ejection fraction, HLD – hyperlipidemia, HTN – hypertension, LAVi – left atrial volume index, pEF – preserved left ventricular ejection fraction, LVMi – left ventricular mass index, TRV – tricuspid regurgitation peak velocity

4.1.3 Individualized patient predictions

Individualized patient predictions for clinical stages, severity, and future adverse events were tested in the secondary cohort. After predicting the region membership of patients of this cohort using a random forest classifier, the same tendency was observed for the probability of MACE-related rehospitalization in the regions as in the primary cohort (Figure 2C). A correlation between NYHA functional classes and ACC/AHA stages with regions was also observed ($\gamma = 0.56$ and $\gamma = 0.67$; both $p < 0.001$, respectively), which indicated that more symptomatic patients were found in the 4th region than in other regions.

We also wanted to demonstrate whether changing the location of a patient on the loop was associated with worsening or improvement of cardiac function. To illustrate the motion of patients on the loop, the predicted regions of the 1st and 2nd echocardiograms were compared. Both echocardiograms in 13 patients were in low-risk regions (region I or II), whereas those in

63 patients were in the high-risk region (region III or IV). Fifteen patients showed improvement (moved from region III and/or IV to region I and/or II) in echocardiographic results, and 5 patients showed worsening (moved from region I and/or II to region II and/or IV) echocardiographic results. Improvement or staying in the low-risk regions was associated with lower MACE-related rehospitalization rates following the second echocardiogram than worsening or staying in high-risk regions (3% vs. 37%, $p < 0.001$).

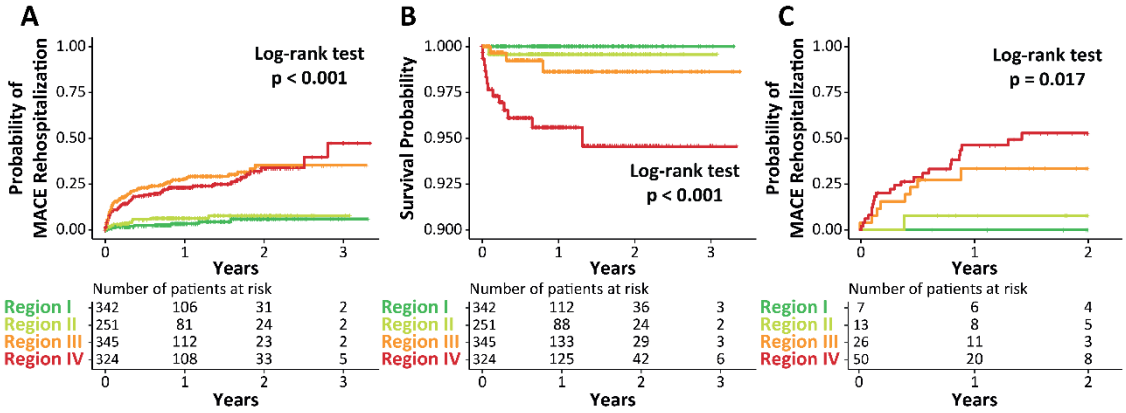

Figure 2 *Kaplan-Meier curves for MACE-related outcomes by regions*

Kaplan-Meier curves of the four regions: (A) MACE-related rehospitalization in the primary cohort, (B) MACE-related death in the primary cohort, and (C) MACE-related rehospitalization in the secondary cohort.

MACE – major adverse cardiovascular event

4.2 Designing and evaluating a machine learning-based risk stratification system to predict all-cause mortality of patients undergoing CRT implantation

4.2.1 Baseline clinical characteristics

The final training cohort included 1,510 patients (75.6% males, 50.8% ischemic etiology, 45.6% CRT-D) who underwent CRT implantation. A total of 158 CRT patients (80.4% males, 60.2% ischemic etiology, 20.3% CRT-D) were prospectively enrolled and entered into the test database. During the 5-year follow-up period, 805 (53.3%) patients died in the training cohort, and there were 80 (50.6%) deaths in the test cohort.

4.2.2 Prediction of all-cause mortality

Among the evaluated ML classifiers, random forest (i.e., the SEMMELWEIS-CRT score) yielded the highest AUCs for predicting all-cause mortality at 1-, 2-, 3-, 4-, and 5-year follow-up in the test cohort. When compared with the pre-existing risk scores, the SEMMELWEIS-CRT score demonstrated significantly better response prediction and greater discrimination of mortality (Table 1).

Table 1 *Area under the receiver operating characteristic curve of the different scores*

	1-year	2-year	3-year	4-year	5-year	Mean
SEMMELWEIS-CRT	0.768 (0.674-0.861)	0.793 (0.718-0.867)	0.785 (0.711-0.859)	0.776 (0.703-0.849)	0.803 (0.733-0.872)	0.785
SHFM	0.537 (0.426-0.647)*	0.543 (0.445-0.642)*	0.539 (0.447-0.632)*	0.544 (0.453-0.635)*	0.544 (0.454-0.634)*	0.541
EAARN	0.602 (0.505-0.699)*	0.627 (0.539-0.714)*	0.653 (0.570-0.736)*	0.649 (0.566-0.731)*	0.643 (0.560-0.726)*	0.635
VALID-CRT	0.529 (0.416-0.643)*	0.618 (0.523-0.713)*	0.638 (0.552-0.725)*	0.637 (0.550-0.724)*	0.650 (0.564-0.737)*	0.614
CRT-score	0.722 (0.637-0.806)	0.743 (0.667-0.818)	0.732 (0.657-0.807)	0.720 (0.644-0.795)	0.693 (0.615-0.771)*	0.722
ScREEN	0.595 (0.516-0.673)*	0.555 (0.477-0.633)*	0.536 (0.460-0.612)*	0.525 (0.449-0.601)*	0.549 (0.474-0.624)*	0.552

**p < 0.05 vs. SEMMELWEIS-CRT, DeLong test. Cell contents are areas under the receiver operating characteristic curves with 95% confidence intervals.*

SHFM – Seattle Heart Failure Model

4.2.3 Machine learning-based risk stratification

Based on the predicted probability of death, patients were split into four quartiles at each year of follow-up. As depicted by Kaplan–Meier curves, there was a significant difference in the distribution of events across the quartiles at all years (Figure 3).

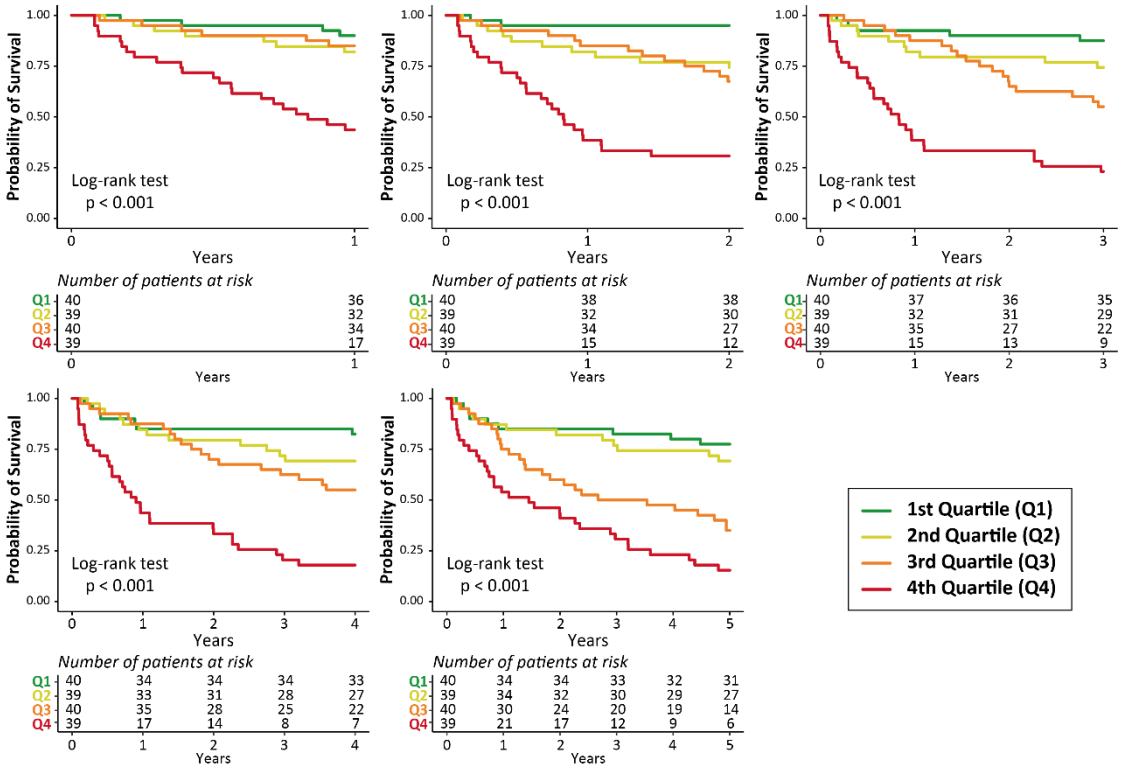

Figure 3 *Survival analysis of the quartiles*

Based on the predicted probability of death, patients were split into four quartiles at each year of follow-up. The survival of the quartiles was visualized on Kaplan–Meier curves, and log-rank tests were performed for comparison.

4.3 Exploring the sex-specific differences and similarities in the predictors of mortality among patients undergoing CRT implantation

4.3.1 Baseline clinical characteristics and all-cause mortality

The final 1- and 3-year cohorts included 2,191 (74.7% males, 50.4% ischemic etiology, 56.7% CRT-D) and 1,900 patients (75.0% males, 51.5% ischemic etiology, 54.1% CRT-D), respectively. In the 1-year cohort, 203 (12.4%) men and 49 (8.8%) women died during the 1-year follow-up period. Univariable Cox regression analysis revealed a significantly lower risk of all-cause mortality in women compared to men (HR: 0.698, 95% CI: 0.511 – 0.954; $p = 0.024$); however, after adjusting for age, etiology of HF, QRS morphology, type of the implanted device, and type of atrial fibrillation (AF), we could not observe a significant difference between sexes (HR: 0.803, 95% CI: 0.581 – 1.110; $p = 0.183$). Males exhibited significantly higher mortality rates compared to females in the 3-year cohort as well (502 [35.2%] vs. 113 [23.8%]; $p < 0.001$). The univariable Cox regression analysis also confirmed this finding as it showed a significantly lower risk of all-cause mortality in females compared to males (HR: 0.625, 95% CI: 0.510 – 0.767; $p < 0.001$). Moreover, this difference remained significant even after adjusting for the previously listed covariates (HR: 0.686, 95% CI: 0.555 – 0.848; $p < 0.001$).

4.3.2 Machine learning for the prediction of 1- and 3-year all-cause mortality

Among the evaluated ML classifiers, CIRF exhibited the best performance for discrimination between survival/all-cause death with an AUC of 0.717 (95% CI: 0.676 – 0.758) and 0.739 (95% CI: 0.715 – 0.762) in the 1- and 3-year training cohorts, respectively. When evaluating the models' discriminatory power in the test cohorts, we observed an AUC of 0.728 (95% CI: 0.645 – 0.802) and 0.732 (95% CI: 0.681 – 0.784) for the prediction of 1- and 3-year mortality, respectively. Models were also trained and tested separately in the female and male subsets of the 1- and 3-year cohorts. The AUCs ranged from 0.712 to 0.748 in the training sets and from 0.681 to 0.798 in the test sets suggesting a modest variability in the models' predictive capabilities across the different subsets of patients.

4.3.3 Most important predictors of mortality as assessed using machine learning

In the overall study population (including both sexes), the most important predictor of 1-year mortality was serum sodium, which was followed by serum creatinine, hemoglobin concentration, age, and etiology of HF (Figure 4). These features were also found among the

strongest predictors of 3-year mortality, however, in different order of importance (serum sodium, age at implantation, hemoglobin concentration, serum creatinine, and etiology).

We observed several sex-specific differences during the subgroup analysis. In males, the top predictors of 1-year mortality were hemoglobin concentration, serum sodium, serum creatinine, left bundle branch block morphology, and age, whereas, in females, the most important predictors were serum sodium, etiology, LVEF, age, and serum creatinine (Figure 4).

In males, the strongest determinants of 3-year mortality were serum sodium, hemoglobin concentration, age at implantation, serum creatinine, and allopurinol, whereas, in females, these features were serum sodium, age at implantation, type of AF, NYHA functional class, and etiology in decreasing order (Figure 4).

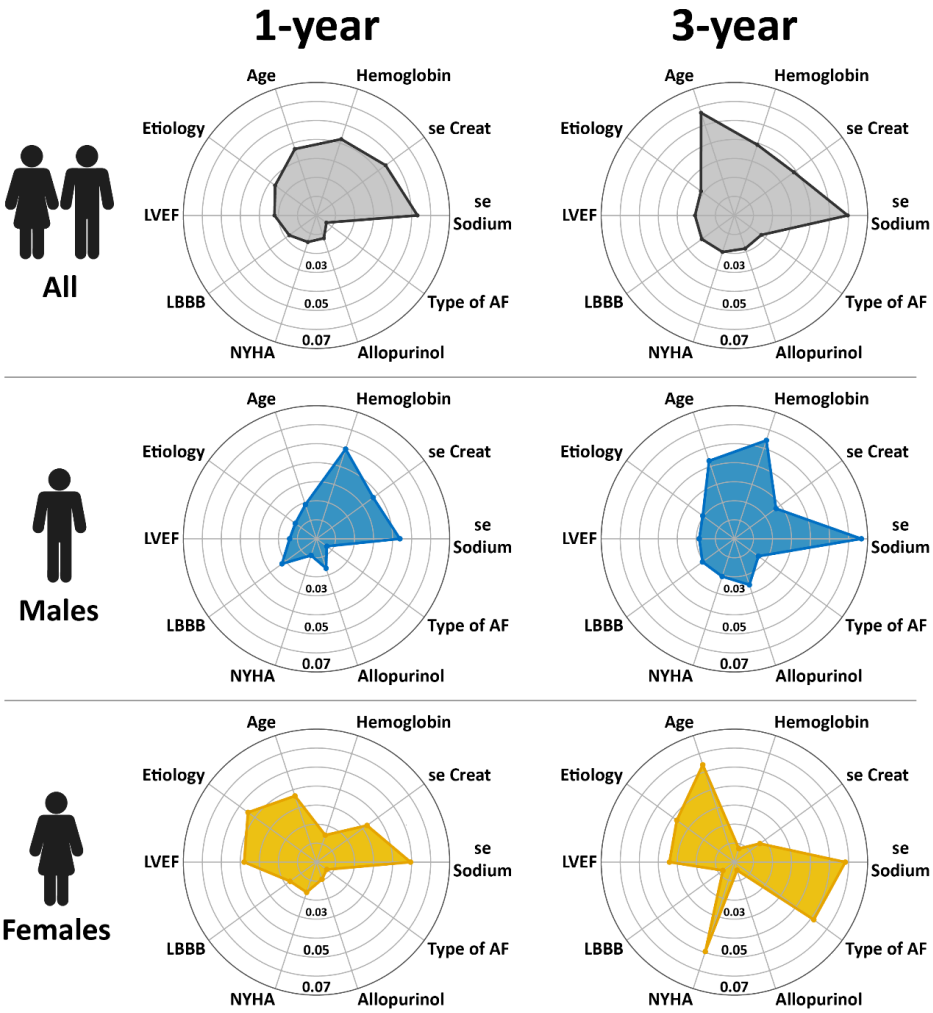

Figure 4 *The most important predictors of 1- and 3-year all-cause mortality in patients undergoing CRT implantation*

To keep the data comparable between the different models, we identified the top 5 predictors in each model and took the union of these features; then, we plotted the results on radar charts.

AF – atrial fibrillation, LBBB – left bundle branch block, LVEF – left ventricular ejection fraction, NYHA – New York Heart Association

5. CONCLUSIONS

1. Based on our first study, in which we applied TDA to analyze the retrospectively and prospectively collected echocardiographic data of a large patient cohort with varying degrees of LV structural and functional remodeling, we reached the following conclusions:
   1.1 TDA is a robust data analytical approach that is capable of effectively integrating multiple echocardiographic parameters of LV structure and function into a looped patient-patient similarity network in which subjects could be mapped to specific locations associated with distinct disease stages and clinical outcomes.
   1.2 TDA can be utilized to trace the progression of cardiac dysfunction in patients as they travel through cycles of compensation and decompensation within a looped disease space.
2. In our second study, in which we implemented and evaluated various ML algorithms to predict all-cause mortality in patients undergoing CRT implantation, we came to the following conclusions:
   2.1 By capturing the non-linear associations between predictors and outcomes, our CIRF-based risk stratification system – the SEMMELWEIS-CRT score – achieved high performance in predicting 1-, 2-, 3-, 4-, and 5-year all-cause death in patients undergoing CRT implantation and effectively outlined patient subgroups at high risk for mid-term and long-term mortality.
   2.2 The SEMMELWEIS-CRT score outperformed several conventional statistics-based risk scores.
3. Our third study, in which we used ML algorithms to explore the sex-specific differences and similarities in the predictors of all-cause mortality among patients undergoing CRT, led us to the following conclusions:
   3.1 Female sex was found to be associated with significantly better survival rates in our cohort of CRT patients.
   3.2 Using CIRF in combination with easily obtainable clinical features, we could effectively predict 1- and 3-year all-cause mortality in patient subsets containing males or females exclusively.
   3.3 Sex-specific patterns were identified in the predictors of mortality, which also changed over time. The role of HF etiology, NYHA functional class, and LVEF was more pronounced in females, whereas hemoglobin concentration, QRS morphology, and treatment with allopurinol were notably more predictive for all-cause mortality in males.

6. BIBLIOGRAPHY OF THE CANDIDATE

6.1 Bibliography related to the present thesis

1. **Tokodi M**, Shrestha S, Bianco C, Kagiyama N, Casaclang-Verzosa G, Narula J, Sengupta PP
   Interpatient similarities in cardiac function: a platform for personalized cardiovascular medicine
   JACC Cardiovasc Imaging 2020;**13**(5): 1119-1132.
   DOI: 10.1016/j.jcmg.2019.12.018
   *IF: **14.805***

2. **Tokodi M***, Schwertner WR*, Kovács A, Tősér Z, Staub L, Sárkány A, Lakatos BK, Behon A, Boros AM, Perge P, Kutyifa V, Széplaki G, Geller L, Merkely B, Kosztin A
   Machine learning-based mortality prediction of patients undergoing cardiac resynchronization therapy: the SEMMELWEIS-CRT score
   Eur Heart J 2020;**41**(18): 1747-1756.
   DOI: 10.1093/eurheartj/ehz902
   **Márton Tokodi, M.D. and Walter R. Schwertner, M.D. are joint first authors.*
   *IF: **29.983***

3. **Tokodi M***, Behon A*, Merkel ED, Kovács A, Tősér Z, Sárkány A, Csákvári M, Lakatos BK, Schwertner WR, Kosztin A, Merkely B
   Sex-specific patterns of mortality predictors among patients undergoing cardiac resynchronization therapy: a machine learning approach
   *Front Cardiovasc Med 2021;**8**: 611055.*
   DOI: 10.3389/fcvm.2021.611055
   **Márton Tokodi, M.D. and Anett Behon, M.D. are joint first authors.*
   *IF (2020): **6.050***

6.2 Bibliography not related to the present thesis

1. Lakatos BK, Tősér Z, **Tokodi M**, Doronina A, Kosztin A, Muraru D, Badano LP, Kovács A, Merkely B
Quantification of the relative contribution of the different right ventricular wall motion components to right ventricular ejection fraction: the ReVISION method
Cardiovasc Ultrasound 2017;**15**(1): 8. DOI: 10.1186/s12947-017-0100-0
*IF: **1.652***

2. Lakatos BK, **Tokodi M**, Assabiny A, Tősér Z, Kosztin A, Doronina A, Rácz K, Koritsánszky KB, Berzsenyi V, Németh E, Sax B, Kovács A, Merkely B
Dominance of free wall radial motion in global right ventricular function of heart transplant recipients
Clin Transplant 2018;**32**(3): e13192. DOI: 10.1111/ctr.13192
*IF: **1.667***

3. Mátyás C, Kovács A, Németh BT, Oláh A, Braun S, **Tokodi M**, Barta BA, Benke K, Ruppert M, Lakatos BK, Merkely B, Radovits T
Comparison of speckle-tracking echocardiography with invasive hemodynamics for the detection of characteristic cardiac dysfunction in type-1 and type-2 diabetic rat models
Cardiovasc Diabetol 2018;**17**(1): 13. DOI: 10.1186/s12933-017-0645-0
*IF: **5.948***

4. Doronina A, Édes IF, Újvári A, Kántor Z, Lakatos BK, **Tokodi M**, Sydó N, Kiss O, Abramov A, Kovács A, Merkely B
The female athlete's heart: comparison of cardiac changes induced by different types of exercise training using 3D echocardiography
Biomed Res Int 2018;**2018**: 3561962. DOI: 10.1155/2018/3561962
*IF: **2.197***

5. Lakatos BK, Kiss O, **Tokodi M**, Tősér Z, Sydó N, Merkely G, Babity M, Szilágyi M, Komócsin Z, Bognár C, Kovács A, Merkely B
Exercise-induced shift in right ventricular contraction pattern: novel marker of athlete's heart?
Am J Physiol Heart Circ Physiol 2018;**315**(6): H1640-H1648. DOI: 10.1152/ajpheart.00304.2018
*IF: **4.048***

6. Oláh A, Kovács A, Lux A, **Tokodi M**, Braun S, Lakatos BK, Mátyás C, Kellermayer D, Ruppert M, Sayour AA, Barta BA, Merkely B, Radovits T
Characterization of the dynamic changes in left ventricular morphology and function induced by exercise training and detraining
Int J Cardiol 2019;**277**: 178-185. DOI: 10.1016/j.ijcard.2018.10.092
*IF: **3.229***

7. Casaclang-Verzosa G, Shrestha S, Khalil MJ, Cho JS, **Tokodi M**, Balla S, Alkhouli M, Badhwar V, Narula J, Miller JD, Sengupta PP
Network tomography for understanding phenotypic presentations in aortic stenosis
JACC Cardiovasc Imaging 2019;**12**(2): 236-248. DOI: 10.1016/j.jcmg.2018.11.025
*IF: **12.740***

8. Kovács A, Lakatos B, **Tokodi M**, Merkely B
Right ventricular mechanical pattern in health and disease: beyond longitudinal shortening
*Heart Fail Rev 2019;**24**(4): 511-520.* DOI: 10.1007/s10741-019-09778-1
*IF: **3.538***

9. Lakatos BK, Molnár AÁ, Kiss O, Sydó N, **Tokodi M**, Solymossi B, Fábián A, Dohy Z, Vágó H, Babity M, Bognár C, Kovács A, Merkely B
Relationship between cardiac remodeling and exercise capacity in elite athletes: incremental value of left atrial morphology and function assessed by three-dimensional echocardiography
J Am Soc Echocardiogr 2020;**33**(1): 101-109.e1. DOI: 10.1016/j.echo.2019.07.017
*IF: **5.251***

10. **Tokodi M**, Németh E, Lakatos BK, Kispál E, Tősér Z, Staub L, Rácz K, Soltész Á, Szigeti S, Varga T, Gál J, Merkely B, Kovács A
Right ventricular mechanical pattern in patients undergoing mitral valve surgery: a predictor of post-operative dysfunction?
ESC Heart Failure 2020;**7**(3): 1246-1256. DOI: 10.1002/ehf2.12682
IF: ***4.411***

11. Lakatos BK, Nabeshima Y, **Tokodi M**, Nagata Y, Tősér Z, Otani K, Kitano T, Fábián A, Újvári A, Boros AM, Merkely B, Kovács A, Takeuchi M
Importance of non-longitudinal motion components in right ventricular function: 3D echocardiographic study in healthy volunteers
J Am Soc Echocardiogr 2020;**33**(8): 995-1005.e1. DOI: 10.1016/j.echo.2020.04.002
IF: ***5.251***

12. Ruppert M, Lakatos BK, Braun S, **Tokodi M**, Karime C, Oláh A, Sayour AA, Hizoh I, Barta BA, Merkely B, Kovács A, Radovits T
Longitudinal strain reflects ventriculo-arterial coupling rather than mere contractility in rat models of hemodynamic overload-induced heart failure
J Am Soc Echocardiogr 2020;**33**(10): 1264-1275.e4. DOI: 10.1016/j.echo.2020.05.017
IF: ***5.251***

13. Ujvári A, Lakatos BK, **Tokodi M**, Fábián A, Merkely B, Kovács A
Evaluation of left ventricular structure and function using 3D echocardiography
J Vis Exp 2020(164). DOI: 10.3791/61212
IF: ***1.355***

14. Lakatos BK, **Tokodi M**, Kispál E, Merkely B, Kovács A
Morphological and functional assessment of the right ventricle using 3D echocardiography
J Vis Exp 2020(164). DOI: 10.3791/61214
IF: ***1.355***

15. Fábián A, Lakatos BK, **Tokodi M**, Kiss AR, Sydó N, Csulak E, Kispál E, Babity M, Szűcs A, Kiss O, Merkely B, Kovács A
Geometrical remodeling of the mitral and tricuspid annuli in response to exercise training: a 3-D echocardiographic study in elite athletes
*Am J Physiol Heart Circ Physiol 2021;**320**(5): H1774-H1785.* DOI: 10.1152/ajpheart.00877.2020
IF (2020): ***4.733***

16. Lakatos BK, Ruppert M, **Tokodi M**, Oláh A, Braun S, Karime C, Ladányi Z, Sayour AA, Barta BA, Merkely B, Radovits T, Kovács A
Myocardial work index: a marker of left ventricular contractility in pressure- or volume overload-induced heart failure
*ESC Heart Fail 2021;**8**(3): 2220-2231.* DOI: 10.1002/ehf2.13314
IF (2020): ***4.411***

17. **Tokodi M**, Levente S, Budai Á, Lakatos BK, Csákvári M, Suhai FI, Szabó L, Fábián A, Vágó H, Tősér Z, Merkely B, Kovács A
Partitioning the right ventricle into 15 segments and decomposing its motion using 3D echocardiography-based models: the updated ReVISION method
*Front Cardiovasc Med 2021;**8**: 622118.* DOI: 10.3389/fcvm.2021.622118
IF (2020): ***6.050***

18. **Tokodi M**, Lakatos BK, Ruppert M, Fábián A, Oláh A, Sayour AA, Ladányi Z, Soós A, Merkely B, Sengupta PP, Radovits T, Kovács A
Left ventricular pressure-strain-volume loops for the noninvasive assessment of volume overload-induced myocardial dysfunction
*JACC Cardiovasc Imaging 2021;**14**(9):1868-1871.* DOI: 10.1016/j.jcmg.2021.03.005
IF (2020): ***14.805***

19. Pandey A, Kagiyama N, Yanamala N, Segar MW, Cho JS, **Tokodi M**, Sengupta PP
Deep-learning models for the echocardiographic assessment of diastolic dysfunction
*JACC Cardiovasc Imaging 2021;**14**(10):1887-1900.* DOI: 10.1016/j.jcmg.2021.04.010
*IF (2020): **14.805***

20. Schwertner WR, Behon A, Merkel ED, **Tokodi M**, Kovács A, Zima E, Osztheimer I, Molnár L, Király Á, Papp R, Gellér L, Kuthi L, Veres B, Kosztin A, Merkely B
Long-term survival following upgrade compared with de novo cardiac resynchronization therapy implantation: a single-centre, high-volume experience
*Europace 2021;**23**(8):1310-1318.* DOI: 10.1093/europace/euab059
*IF (2020): **5.214***

21. **Tokodi M**, Oláh A, Fábián A, Lakatos BK, Hizoh I, Ruppert M, Sayour AA, Barta BA, Kiss O, Sydó N, Csulak E, Ladányi Z, Merkely B, Kovács A, Radovits T
Novel insights into the athlete's heart: is myocardial work the new champion of systolic function?
Eur Heart J Cardiovasc Imaging 2021. DOI: 10.1093/ehjci/jeab162
*IF (2020): **6.875***

22. Molnár AÁ, Kolossváry M, Lakatos BK, **Tokodi M**, Tárnoki ÁD, Tárnoki DL, Kovács A, Szilveszter B, Vörös S, Jermendy G, Maurovich-Horvat P, Merkely B
Left ventricular systolic function has strong independent genetic background from diastolic function: a classical twin study
*Medicina 2021;**57**(9): 935.* DOI: 10.3390/medicina57090935
*IF (2020): **2.430***

23. Csulak E, Petrov Á, Kováts T, **Tokodi M**, Lakatos BK, Kovács A, Staub L, Suhai FI, Szabó EL, Dohy Z, Vágó H, Becker D, Müller V, Sydó N, Merkely B
The impact of COVID-19 on the preparation for the Tokyo Olympics: a comprehensive performance assessment of top swimmers
*Int. J. Environ. Res. Public Health 2021;**18**(18): 9770.* DOI: 10.3390/ijerph18189770
*IF (2020): **3.390***

24. Surkova E, Kovács A, **Tokodi M**, Lakatos BK, Merkely B, Muraru D, Ruocco A, Parati G, Badano LP
Contraction patterns of the right ventricle associated with different degrees of left ventricular systolic dysfunction
Circ Cardiovasc Imaging 2021. DOI: 10.1161/CIRCIMAGING.121.012774
*IF (2020): **7.792***

Hungarian articles:

1. Lakatos BK, Kovács A, **Tokodi M**, Doronina A, Merkely B
[Assessment of the right ventricular anatomy and function by advanced echocardiography: pathological and physiological insights]
Orv Hetil 2016;**157**(29): 1139-46. DOI: 10.1556/650.2016.30491 *IF: **0.349***

2. Ujvári A, Komka Z, Kántor Z, Lakatos BK, **Tokodi M**, Doronina A, Babity M, Bognár C, Kiss O, Merkely B, Kovács A
[3D echocardiographic analysis of elite kayak/canoe athletes]
Cardiol Hung 2018;**48**(1): 13-19. DOI: 10.26430/CHUNGARICA.2018.48.1.13

3. Fábián A, Lakatos BK, Kiss O, Sydó N, Vágó H, Czimbalmos C, **Tokodi M**, Kántor Z, Bognár C, Major D, Kovács A, Merkely B
[Functional shift of right ventricular mechanics in athletes: a three-dimensional echocardiography study]
Cardiol Hung 2019;**49**(1): 17-23. DOI: 10.26430/CHUNGARICA.2019.49.1.17

4. Parázs N, Lakatos BK, Kovács A, Assabiny A, Király Á, Tarjányi Z, Szakál-Tóth Z, Teszák T, **Tokodi M**, Ujvári A, Kugler S, Szücs N, Merkely B, Sax B
[Right heart failure many years after heart transplantation – a case of a rare etiology]
Cardiol Hung 2021;**51**(1): 69-72. DOI: 10.26430/CHUNGARICA.2021.51.1.69